INVESTIGATION OF MULTI-ZONE MODELS FOR SPARK IGNITION ENGINE FUELED WITH ETHANOL

Olatunde Bilikis Olanrewaju[1*], Dare Adebukola Ademola[2], Ismail Olawale Saheed[2], Shote Adeola Suhud[1], Alamu Oguntola Jelili[3] and Sulaiman Adedoyin Musediq[1]

[1]Department of Mechanical Engineering, Olabisi Onabanjo University Ago Iwoye, Nigeria
[2]Department of Mechanical Engineering, University of Ibadan, Nigeria
[3]Department of Mechanical Engineering, Osun State University, Nigeria

[*]Corresponding author: olatunde.bilikis@oouagoiwoye.edu.ng

ABSTRACT: This research is aimed at investigating the effect of using ethanol (E100) in multi-zone model analysis consisting of multi-combustion chamber zoning cases. The first case considered is a three-zone model that has an unburned zone, burned zone, and transitory zone. The second case model is also three-zone, consisting of an unburned zone and two partitioned burned zones. The burned zone was imagined partitioned into burned zone-1 and burned zone-2 under uneven fuel distribution having different equivalent ratios. The third case is a four-zone model including two regions of burned zone, an unburned zone and a transitory zone, which is unburned burned zone containing a mixture of unburned and burned gases. Arbitrary constants for each of the unburned (CC1) and burned (CC2) Zone leakages in the unburned burned Zone are 0.00025, 0.0005, 0.001, 0.002, 0.005, 0.1 and 0.5. The Mass Fraction Burned (MFB) for zone-1, x1 and burned zone-2, x2 are computed using Partitioned Burnt Zones Ratios (PBZR) of 2:8, 3:7, 4:6, 5:5, 6:4, 7:3 and 8:2. Two equivalent ratios, one for each fuel MFB (ϕ1, ϕ2), (0.8, 0.6) and (0.6, 0.8) are analyzed using fuel blends of varying percentage. A comparison of values of the three zoning cases is done using peak values from the three-zone models to evaluate the four-zone model. The model was compared with a spark ignition engine (SIE) operating with a premium motor spirit (PMS) serving as baseline. The engine operating conditions were set at an engine speed of 2000 rpm, -35bTDC ignition time, and burn duration at 60 ºC. The indicated mean effective pressure (IMEP), thermal efficiency (η), cylinder pressure and emission fraction from the developed models and those of two-zone analysis obtained agreed with literature values. The result showed it is undesirable to have a high volume of burned charge as infiltrate. The three-zone segmented model predicted the highest engine thermal efficiency and peak pressure at mass burn ratio of 7:3. A general reduction in N_2 emission was observed for the three-zone transitional and four-zone models.

ABSTRAK: Kajian ini menilai kesan etanol (E100) dalam analisis model zon-berbilang yang terdapat pada masalah pengezonan kebuk pembakaran-berbilang. Kes pertama yang diambil kira adalah model tiga-zon yang mempunyai zon tidak terbakar, zon terbakar dan zon peralihan. Model kedua merupakan juga tiga-zon yang terdiri daripada zon tidak-terbakar dan dua zon bahagian yang terbakar. Zon yang terbakar dibahagikan kepada zon-1 terbakar dan zon-2 terbakar di bawah kebakaran tidak sekata yang mempunyai nisbah berlainan. Kes ketiga adalah model zon-keempat termasuk dua kawasan zon terbakar, zon tidak-terbakar dan zon peralihan iaitu zon terbakar tidak-terbakar di mana ia adalah campuran gas terbakar dan tidak-terbakar. Tetapan sebarangan bagi setiap zon kebocoran tidak-terbakar (CC1) dan terbakar (CC2) dalam zon terbakar tidak-terbakar adalah 0.00025, 0.0005, 0.001, 0.002, 0.005, 0.1 dan 0.5.

Pecahan Jisim Terbakar (MFB) bagi zon-1, x1 dan zon-2 terbakar, x2 dikira menggunakan Nisbah Zon Bahagian Terbakar (PBZR) sebanyak 2:8, 3:7, 4:6, 5:5, 6:4, 7:3 dan 8:2. Nisbah dua persamaan, setiap satu bahan api MFB adalah (φ1, φ2), (0.8, 0.6) dan (0.6, 0.8) dan diuji menggunakan pelbagai peratus bahan api campuran. Nilai perbandingan bagi tiga kes zon dibuat menggunakan nilai puncak dari model tiga-zon bagi menilai model empat-zon. Model ini dibandingkan dengan enjin cucuhan bunga api (SIE) beroperasi dengan motor alkohol premium (PMS) sebagai garis asas. Keadaan operasi enjin adalah dihadkan pada 2000 rpm kelajuan enjin, masa pencucuhan -35bTDC dan tempoh pembakaran pada 60 °C. Tekanan berkesan min tertunjuk (IMEP), kecekapan haba tertunjuk (η), tekanan silinder dan pecahan pengeluaran dari model yang dibangunkan dan analisis dua-zon yang terhasil adalah sama dengan nilai literatur. Dapatan kajian menunjukkan cas terbakar pada isipadu yang banyak adalah tidak diingini sebagai penyerap. Model tiga bahagian zon menunjukkan kecekapan haba enjin tertinggi dan tekanan puncak pada jisim bakar dengan nisbah 7:3. Manakala, pengurangan umum telah diperhatikan pada pengeluaran N_2 di peralihan tiga-zon dan model empat zon.

---

1. INTRODUCTION

Modification and optimization of combustion chamber geometry has been seen as the end game in achieving stringent emission reduction and better engine performance with several researches conducted and some ongoing. Researchers have reported the importance of engine combustion chamber modification and its ability to resolve complications arising from adopting some other methods of engine optimization [1-2]. Efforts at combustion chamber modification by [3] was aimed at correcting the lean burn effect, the design modification was carried out for two compression ratios 10 and 11 which necessitated variation in piston bowl size from 16mm to 13.6mm. Increased compression ratio from 10 to 11 was reported to have resulted in leaner combustion but adversely higher combustion duration and coefficient of variance necessitating development of a new combustion chamber design. The modified combustion bowl by [3] has six leaves placed eccentrically to create the desired swirl breakup with a cutout for the inlet and exhaust valve seats. The difference in diameter between the inner and outer bowl was reduced to improve flame propagation and strengthen squish effect.

More researches on modification of the combustion chamber for the purpose of promoting faster burning of charge in a lean burn engine by using the swirl and squish principles was carried out by [2] and [4]. A chamber modification similar to the one described by [3] is the Nebula chamber, employed to retard the swirl motion close to TDC. The Nebula combustion chamber used by [5] is such that the bowl shape forces the swirl to develop into colliding air flows thereby creating the desired great turbulence and fast burn effect. [6] went a step further by implementing the Squish, Nebula, and another named Tokyo Gas, TG with similar purpose as the Nebula but different in that the TG was described as having "a cylindrical dent with semi-circular slants oppositely shaped". The resulting effect of the TG is large turbulence at the cylinder wall and weak turbulence in the center of the cylinder to stabilize flame ignition. The Nebula, TG and squish were reported to have achieved NO_x reduction, increased thermal efficiency and stable combustion. [7-8], adopted ten different combustion chamber geometries in studying the effect of chamber geometry on flow, combustion, and emissions. Of all the geometries studied by [7-8], the cylindrical and square bowl gave the expected turbulence. However, the cylindrical bowl has desired outcome of its peak turbulence close to TDC. The

experiment further confirmed that combustion chamber shape has an effect on flow field, heat release rates, and emission rate. Use of simulation model has been proven to be a cost effective and efficient way of optimizing engine performance and emissions. In [9], three different approaches for combustion modeling in SI engines were identified, while the multi-zone approach to engine modeling seemed the cheapest, fastest and yet efficient modeling method [10]. In their study, [10] concluded the use of additional zone lead to increased heat release prediction. Furthermore, [11] observed increased engine performance using a three-zone model for predicting the effect of ethanol with diesel fuel. Several researches have been carried out on the use of a modeling approach for optimization of combustion processes. Additionally, there are still continuous environmental challenges that need to be addressed. This desire has necessitated the need for further study.

The attention received by ethanol as an alternative fuel is said to be due to its role in reducing problems such as climate change, depleting fossil oil and high oil prices in the international market. Alcohols like ethanol can be produced by fermentation of different biological feedstocks as reported by [12-13]. The most positive properties of ethanol include its ability to be produced from renewable energy sources, its high-octane number, and its high laminar flame speed [14]. The negative aspects include its low heating value due to higher oxygen content compared to gasoline, and it causes corrosion in the metal and rubber parts of an engine [15]. The engine power improves with ethanol as it has better anti-knock characteristics qualities [16]. The engine power also improves with an increase in compression ratio [17]. Ethanol has a high latent heat of vaporization, the latent heat cools the intake air and hence, increases the density and volumetric efficiency [18]. The lower heating value of ethanol enables it to have a higher compression ratio as compared to gasoline [19]. It is desirable for SI engine to have high octane and low cetane numbers. This implies higher resistance to self-ignition and lower auto-ignition possibility. Ethanol can be used as a fuel in spark ignition engines either in pure form (E100) or blended with premium motor spirit (PMS). The use of pure ethanol implies some problems during cold start due to lower vaporization compared to gasoline, which in some cases should require an electrical preheating of the engine block. The use of ethanol in conventional spark ignition engines comes with the problem of corrosion [20]. One of the problems is tackled by the invention of flexible fuel vehicles (FFVs) which implies that the fuel system is made using stainless steel, with some rubber parts replaced by nylon, fluorinated plastics, and high-density polyethylene [21,22]. The lower heating value (LHV) of ethanol requires an alteration of the injection control to increase the fuel flow [23]. Therefore, only a limited percentage of ethanol, up to 10-25%, is recommended for use in conventional gasoline engines [24]. However, FFVs designed to operate with any gasoline-ethanol mixtures are increasing. The advantage of FFV systems consists of the possibility offered by the control system of the engine to detect the concentration of ethanol in the tank and automatically optimize both injection and ignition [14,25].

According to [21], car manufacturers are capable of making vehicles compatible with hydrated ethanol, E100, at no additional cost. However, some investigation has pointed to the presence of ethanol in higher concentration as the cause of volatile organic matter (VOC) emission in the form of benzene [26]. The point line remains that there is more to be discovered for proper evaluation and optimization of ethanol and ethanol-blended fuel usage. Numerous researches [18,27-29], have been carried out concerning the use of ethanol blends in SI engines, but very few uses of 85-100% ethanol have been documented [21]. [30] investigated the effect of varying ethanol-gasoline blends up to 85% and compared the combustion of gasoline and gasoline-ethanol blends through pressure

analysis. An increase in engine efficiency was observed, coupled with CO_2 emission reduction when ethanol blends were used. This study is aimed at investigating the effect of 100% ethanol, E100 on engine performance using a thermodynamic multi-zone model approach.

2. GENERAL METHODOLOGY

To investigate the combustion process, three multi-zone models were developed, each with peculiar characteristics to study effects of additional zone(s) on spark ignition engine combustion characteristics using ethanol as fuel. The model geometry developed by the authors and adopted in this work was the same used by [31,32], where a zero-dimensional, multi-zone model was investigated. The developed models are validated making use of the model developed by [33], primarily for the two-zone model SI engine using gasoline.

In the analysis for the first multi-zone model, which is a three-zone model consisting of the primary burned and unburned zones in addition to a mixed zone described as the transitory zone, the mass infiltration from either of the primary zones, directly into the transitory zone is given in terms of constants of infiltration as shown in Eq. 1.

$$m_{ub}= CC_1* m_u \text{ and } m_{bu}= CC_2* m_b \tag{1}$$

where CC_1 and CC_2 are the arbitrary constants of infiltration from burned and unburned zones respectively. The second multi-zone case has its burned zone partitioned in two, the mass of the burned zone is imagined partitioned into burned zone-1 and burned zone-2 as the proportion of the mixture is uneven in the chamber and therefore, has different mass burning rates (x1, x2). The coefficients of heat transfer are predetermined to be (h_{400}, h_{450}, h_{500}), the mass fraction burned, is represented analytically as shown in Eq. 2 [34].

$$x = 0.5 * \left(1 - \cos\left(pi * \frac{(\theta - \theta_s)}{\theta_b}\right)\right), \tag{2}$$

where, x is mass fraction burned, θ, θ_s, θ_b are the crank angle, the start of energy release and duration of energy release respectively. Peak results of the two analyses of mass fraction and mass infiltration burned are employed for analysis in the third multi-zone case as a four-zone model.

The indices of performance, thermal efficiency (η), indicated mean effective pressure (IMEP) and emission fractions obtained using the developed models are compared with the standard two-zone model. The engine geometry for the model adopted for validating the developed model codes is shown in Table 1 and all are compared with the experimental data; CFD results obtained by [35] for the first multi-zone case and a four-stroke SIE (EF7) running on CNG [36] for the second multi-zone case.

2.1 Development of Mathematical Models

The first law of thermodynamics is applied to all the zones to develop the model equations. In an open system, the rate of change of mass is equal to the net flux of mass across the boundaries of the system. This is expressed by Eq. 3.

$$m = \sum_k \dot{m}_k \tag{3}$$

The mass flux of the control volume can be expressed as the addition of all unit zones as shown in Eqs. 4-6.

$$m = m_u + m_b + m_{un} \text{ (for first case)} \tag{4}$$

$$m = m_u + m_{b1} + m_{b2} \text{ (for the second case)} \tag{5}$$

$$m = m_u + m_{b1} + m_{b2} + m_{un} \text{ (for the third case)} \qquad (6)$$

From the first law of thermodynamics, the energy equation of an open system is expressed as Eq. 7.

$$\dot{E} = \sum \dot{m}h - \dot{W} + \dot{Q} \qquad (7)$$

Equation 7 is therefore applied to expansion, compression, and combustion phases of the internal combustion (ICE) cycle. The model equations analysed in a computation environment are as shown in Eqs. 8 - 10 for the three modeled cases considered. Detailed mathematical derivation of these equations can be found in [31,32]. Sub-models including, air and fuel data, engine geometry inherent in the two-zone model [33] are also employed to analyze the present models.

Table 1: Engine specifications for validating modeled cases

Parameter	First case model evaluation [35]	2-zone model [33]	Second case model evaluation [36]
Number of cylinder	4	4	4
Bore (m)	0.079	0.1	0.085
Stroke (m)	0.086	0.08	0.078
Compression ratio	16	10	11
Displacement (m)	1.7	-	1.018
Inlet valve close	136BTDC	-	-
Exhaust valve open	122ATDC	-	-
Equivalence ratio	-	0.8	-
Burn duration angle	-	60	-
Start of combustion	-	-35	21
End of combustion	-	-	30
Engine speed (rpm)	1500	1500	2000

2.1.1 Model Equation for the First Case Studied

$$\frac{dP}{d\theta} = \{\frac{V_u}{T_u}\frac{dT_u}{d\theta} + \frac{V_b}{T_b}\frac{dT_b}{d\theta} + \frac{V_{un}}{T_{un}}\frac{dT_{un}}{d\theta} + (v_b - v_u)\frac{dm_{x1}}{d\theta} + (v_{un} - v_u)\frac{dm_{ub}}{d\theta} + (v_{un} - v_b)\frac{dm_{bu}}{d\theta} - v_u\frac{dm_{lu}}{d\theta} - v_b\frac{dm_{lb}}{d\theta} - v_{un}\frac{dm_{lun}}{d\theta} - \frac{dV}{d\theta}\}/\frac{V}{P} \qquad (8)$$

2.1.2 Model Equation for Second Case Studied

$$\frac{dP}{d\theta} = \{\frac{V_u}{T_u}\frac{dT_u}{d\theta} + \frac{V_b}{T_b}\frac{dT_b}{d\theta} + \frac{V_{b2}}{T_{b2}}\frac{dT_{b2}}{d\theta} + (v_b - v_u)\frac{dm_{x1}}{d\theta} + (v_{b2} - v_u)\frac{dm_{x2}}{d\theta} - v_u\frac{dm_{lu}}{d\theta} - v_b\frac{dm_{lb}}{d\theta} - v_{b2}\frac{dm_{lb2}}{d\theta} - \frac{dV}{d\theta}\}/\frac{V}{P} \qquad (9)$$

2.1.3 Model Equation for Third Case Studied

$$\frac{dP}{d\theta} = \{\frac{V_u}{T_u}\frac{dT_u}{d\theta} + \frac{V_b}{T_b}\frac{dT_b}{d\theta} + \frac{V_{b2}}{T_{b2}}\frac{dT_{b2}}{d\theta} + \frac{V_{un}}{T_{un}}\frac{dT_{un}}{d\theta} + (v_b - v_u)\frac{dm_{x1}}{d\theta} + (v_{b2} - v_u)\frac{dm_{x2}}{d\theta} + (v_{un} - v_u)\frac{dm_{ub}}{d\theta} + (v_{un} - v_b)\frac{dm_{bu}}{d\theta} + (v_{un} - v_{b2})\frac{dm_{b2}}{d\theta} - v_u\frac{dm_{lu}}{d\theta} - v_b\frac{dm_{lb}}{d\theta} - v_{b2}\frac{dm_{lb2}}{d\theta} - v_{un}\frac{dm_{lun}}{d\theta} - \frac{dV}{d\theta}\}/\frac{V}{P} \qquad (10)$$

3. MODEL IMPLEMENTATION

3.1 Transitional Model

Relevant sub-programs such as the air and fuel were implemented for the two-zone model. Integration of the governing equations developed using ODE45 in MATLAB code is used to obtain the temperature and pressure distribution for various phases in SI engine operation using ethanol for the computation.

Implementation of the transitional three-zone model is done using selected values of infiltration in the developed code following the steps below;

- Implementing input parameters (available in engine.m)
- Cylinder volume and mass are evaluated
- Determination of relevant thermophysical properties such as u, h, cp, etc.
- Mass fraction burned is evaluated
- Heat transfer coefficient is selected using either constant estimated values or Woschni Equation
- Inputing selected constants for CC_1 and CC_2 using additional program
- Computing the required governing equations.

The model employs the parameters of an ICE with combustion and operating parameters details as stated in Table 1.

3.2 Segmented Model

The mass burned zone is imagined partitioned into burned zone-1 and burned zone-2 since there is a proportion that is unevenly mixed in the chamber and therefore they have different mass burning rates (x1, x2) and heat transfer coefficients, (h_{400}, h_{450}, h_{500}). Mass fraction burned, denoted by x, while, θ, θ_s, θ_b are the crank angle, start of energy release and duration of energy release respectively. These parameters are represented analytically and the equation solved is also presented in Eq. 2.

3.3 Transitional-Segmented Model

In this model, special consideration is given to mass infiltration into the transitory zone and mass fraction ratio such that predetermined optimal results are analyzed for the third case (four-zone model).

4. RESULTS AND DISCUSSION

4.1 Transitional Model (First Case Model)

Figure 1 shows the thermal efficiency (Ƞ), temperature, pressure, and indicated mean effective pressure (MPa) at varying CC_1 while the value of CC_2 (unburnt) is kept constant at 0.001 and at varying CC_2 while the value of CC_1 (burnt) is kept constant at 0.001 are shown in Fig. 1. Highest Ƞ, pressure and IMEP are observed at the least infiltration constant of 0.00025, values of all properties decreased as the infiltration constant increased, an evidenced in the sharp decrease observed from infiltration constant 0.005 to 0.1 for pressure, IMEP and Ƞ. It can be deduced that for the varying CC_1, the least infiltration constant from burnt region to the mixed region of unburnt burned is favorable for all performance parameters and that a greater infiltration has adverse effect on the engine efficiency. Generally, infiltration from the burned zone has greater effect on the

engine performance compared to infiltration from the unburned zone as steeper slopes of Fig. 1 suggest for CC_1 as compared to CC_2. It is observed that the difference in variation witnessed for varying CC_2 is not as steep as it was for varying CC_1 as shown in Fig.1 due to the positive implication of unburnt infiltration into the mixed region until optimum values of engine performance are observed and then a decrease in performance beyond this point is evident. It is also evident that slight backflow of burned charge will have noticeable adverse effect on engine performance while these effects are less noticeable and require a lot more unburned charge to infiltrate into the mixed zone to reduce engine performance. Practically, infiltration in the combustion chamber could be inform of crevice flow and blowby, it is essential to have a limited amount of burned gas as backflow to avoid reduction in power and efficiency as mentioned by [37].

The observed peak pressure (in Table 2) using E100 is 15.7% closer to the experimental data. However, when compared to the 2-zone model it is 16.4% closer to the experimental value. High IMEP and η are also observed for the E100 3-zone model.

In Fig. 2, concerning three-zone and two-zone models, there is no significant difference in the general emission patterns of CO_2, NO, and O_2. A reduction in values of N_2 is observed for the three-zone model which could be attributed to higher oxygen content present in ethanol to react with the N_2.
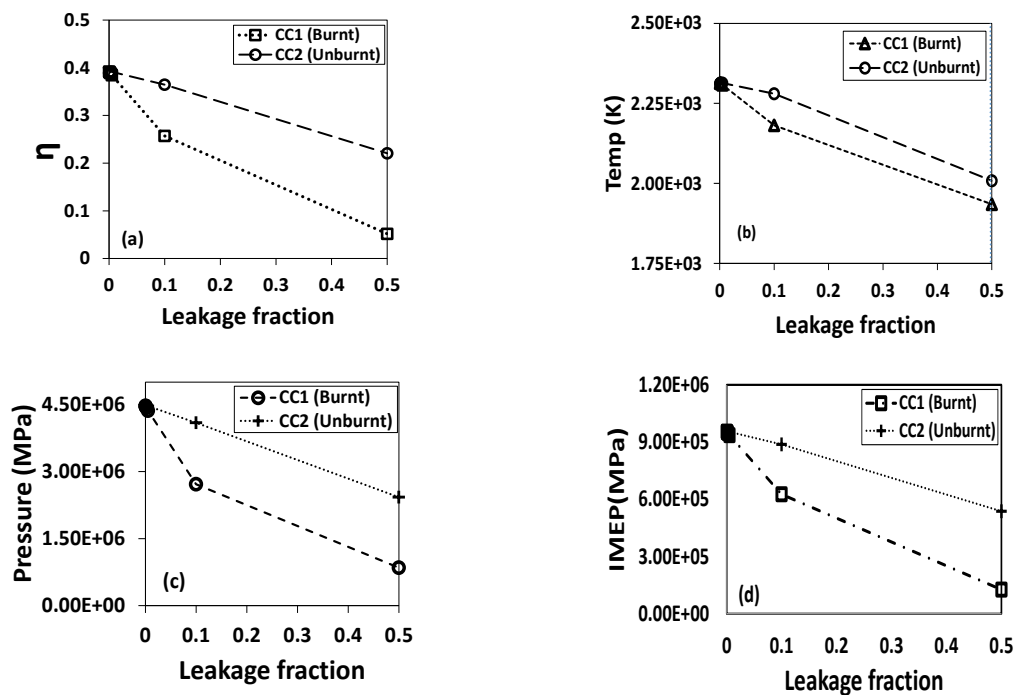

Fig. 1: 3-zone model for the fractional burnt and unburnt regions,
(a) efficiency, (b) temperature, (c) pressure and (d) Indicated Mean Effective Pressure.

Table 2: Comparison of 2-zone model, 3-zone model and experimental results

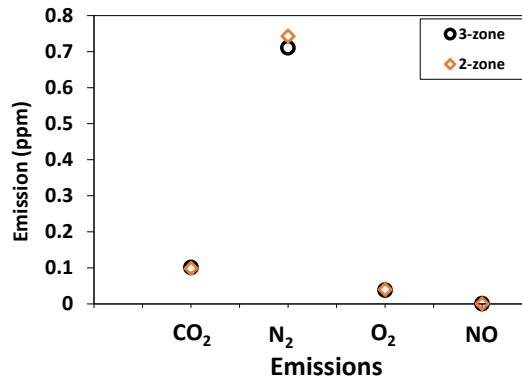|	2-zone model	Experimental values	3-zone model with C_1= 0.00025 and C_2= 0.001	3-zone model at 0.005	3-zone model at optimal value of C_1 = 0.00025 and C_2 = 0.005
Pressure (MPa)	4.4358e+06	5.30E+06	4.4680e+06	4.4668e+06	4.4651e+06
IMEP	9.1635e+05	-	9.5427e+05	9.5382e+05	9.5344e+05
η	0.3741	-	0.3917	0.3915	0.3914

Fig. 2: Emissions for the 2-zone and case-1 models using ethanol.

4.2 Segmented Model

The η, temperature and IMEP history for varying segmented burned zones for E100 investigated are as shown in Fig. 3 using varying heat transfer coefficient as seen in Fig. 3 (a, b, c and d) for heat transfer coefficients, h = 400, 450, and 500, respectively.
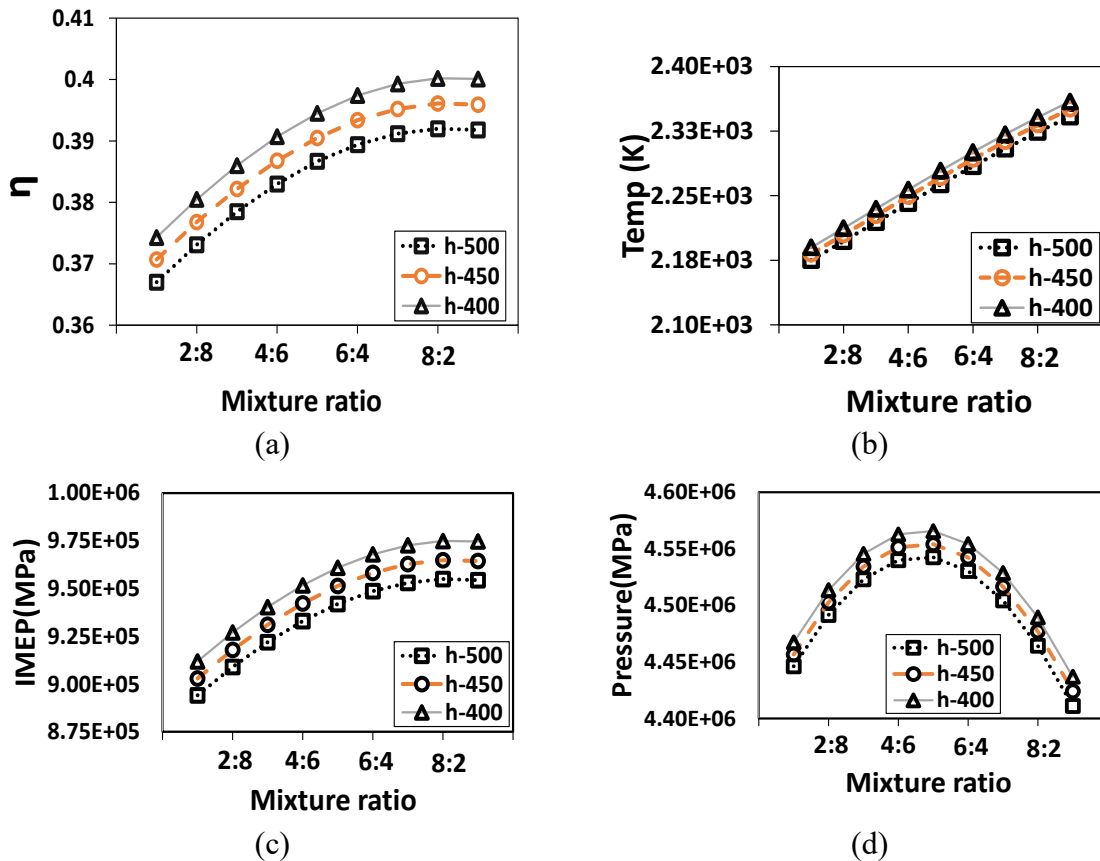

Fig. 3: Three-zone model values for the burned zone-1 and burned zone-2
using heat transfer coefficients 500 and 450 (a) efficiency, (b) temperature,
(c) IMEP and (d) pressure.

The maximum peak pressures in Fig. 3(d) for h_{400}, h_{450}, h_{500} are 4.57 MPa, 4.55 MPa, 4.54 MPa, respectively are observed using 4:6, although the highest thermal efficiency and IMEP are observed at a mixture ratio of >7:3, h_{400} in Fig. 3(a and c). Expectedly, the engine temperature history increased as mass flow rate increased in Fig. 3(b), however, the

peak temperature was observed towards the end of the burn flow. Evidently, a partition in the burned mixture had an effect on the engine performance as an increase in engine performance is observed as the mixture ratio increased. It can be argued that a proper and sequential fair variation in mixture ratio to an optimal ratio can increase the engine performance while a decrease in engine performance is observed beyond the optimal value. It is also worthy of note that the sequence of the segment is important, as a ratio of 8:2 is greater compared to a ratio of 2:8. Therefore, the flow and turbulence in the engine chamber requires uniformity to a certain degree and later a little variation or reduction in flow towards the end of the combustion process to stabilize flame ignition as described by [6].

4.3 Transitional-Segmented Model

The readings from both analyses of mass fraction and mass infiltration burned from cases-1 and 2 respectively are used for the third case. This work has reported findings from combining the optimal results. Table 3 presents the four-zone model results for pressure, IMEP, η and emission fractions analyzed from the optimal mass infiltration and mass fraction burned values. It was observed that there was a reduction in CO_2 and increased N_2 emission fraction for the 4-zone model as compared to the other 3-zone models.

Experimental values, 2-zone, 3-zone, and 4-zone models are shown in Table 4. From the table, higher pressure values observed for the 4-zone model is 3.9% closer to experimental results while that of the 2-zone model is 4.4% closer to the experimental results.

Table 3: 4-zone (third case) modelled using ethanol

CC_1	CC_2	P_e (MPa)	Temp (K)	IMEP	η	CO_2	H_2O	N_2	O_2	NO
0.00025	0.005	4.4651e+06	2.3134e+03	9.5344e+05	0.3914	0.1007	0.1511	0.7104	0.0377	0.0001
X1	X2									
0.7	0.3	4.4893e+06	2.341e+03	9.7492e_05	0.4002	0.1007	0.1511	0.7104	0.0377	0.0001
Case-3 Values		4.4565e+06	2.3344e+03	9.4735e+05	0.3867	0.0983	0.1194	0.7428	0.0395	0.0001

Table 4: Showing comparison of results from 2-zone model,
three cases modeled and experimental results

	2-zone model	Experimental values	3-zone model using X1 = 0.7 and X2 = 0.3	3-zone model using CC_1 = 0.00025 and CC_2 = 0.005	4-zone Model using X1 = 0.7 and X2 = 0.3 (h_{400}), CC_1 = 0.00025 and CC_2 = 0.005
Pe	4.4358e+06	4.640e+06	4.4893e+06	4.4651e+06	4.4565e+06
T_{be}	2305K	2800K	2.3410e+03	2.3134e+03	2.3344e+03
IMEP	9.1635e+05		9.7492e+05	9.5344e+05	9.4735e+05
η	0.3741	-	0.4002	0.3914	0.3867

Table 5 shows comparative analysis using ethanol E100 of the three-zone model involving mass infiltration at optimal values of CC1= 0.00025 and CC2 = 0.005, three-zone model involving mass burn rate of x1 = 0.7 and x2 = 0.3 and a four-zone model labeled as case 3. Emission history for the four-zone model, like the two-zone model, remains the lowest for all emission types. The highest peak pressure, IMEP, and η are observed at the three-zone case 2 model, and this is clearly shown in Fig. 4. It could be concluded that the segmented three-zone model (3zc2) is better for peak in-cylinder pressure and engine efficiency analysis using ethanol, E100. In Fig. 4(a-d), the three-zone

segmented model (3zc2) produces the best results in terms of efficiency, pressure, temperature and IMEP.

Table 5: Comparison of 2-zone, 3-zones (case-1 and case-2)
and 4-zone models (case-3) using ethanol, E100

	Pressure (MPa)	Temp (K)	IMEP	η	Emission characteristics				
					CO_2	H_2O	N_2	O_2	NO
2-zone model, 2z	4.4358e+06	2305K	9.1635e+05	0.3741	0.0983	0.1194	0.7428	0.0395	0.0001
First case, 3zc1 using CC1 = 0.00025 and CC2 = 0.005	4.4651e+06	2.3134e+03	9.5344e+05	0.3914	0.1007	0.1511	0.7104	0.0377	0.0001
Second case, 3zc2 0.7 0.3	4.4893e+06	2.3410e+03	9.7492e+05	0.4002	0.1007	0.1511	0.7104	0.0377	0.0001
Third case, 4z	4.4565+06	2.3344e+03	9.4735e+05	0.3867	0.0983	0.1194	0.7428	0.0395	0.0001

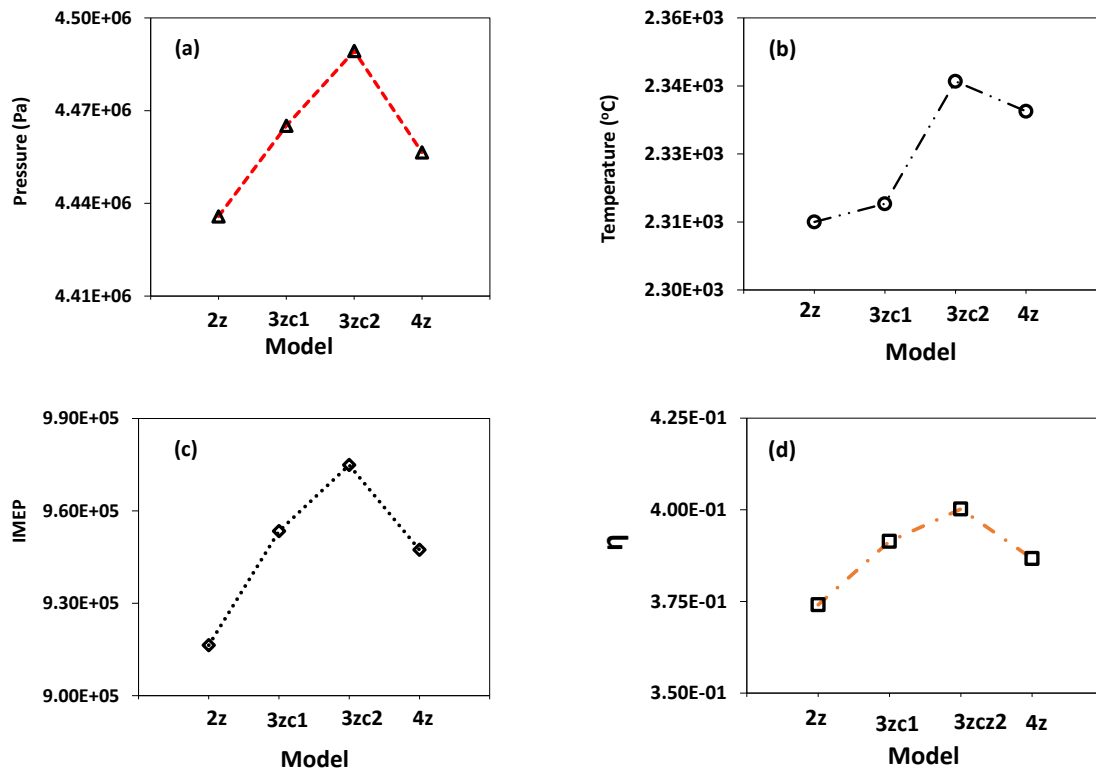2z-2zone model, 3zc1-3zone case 1 model, 3zc2- 3zone case 2 model, 4z- 4zone model

Fig. 4: Temperature, Indicated Mean Effective Pressure (IMEP) and thermal efficiency (η) for 2-zone model (2z), 3-zone transitory model (3zc1), 3-zone segmented model (3zc2) and 4-zone model (4z) using 100% ethanol fuel.

5. CONCLUSIONS

Multi-zone models have been developed for analysis of combustion in spark ignition engines using ethanol as fuel. It is evident that inclusion of additional zones into the combustion chamber analysis and use of ethanol has increased the engine performance in terms of indicated mean effective pressure, thermal efficiency and emission rate. From the developed models and analysis, the following conclusions can be drawn:

1. The infiltration of charges in the combustion chamber should be limited for burned gases as found in the range of infiltration (0.0025, 0.005) that gave optimum values of engine performance for burned and unburned gases respectively.

2. Homogenous flow; creating uniformity of charge flow of ratio 7:3 is encouraged for burned gases.

3. The three-zone segmented model was observed to give a better result of engine performance.

4. Generally, engine zoning has significant effect on engine performance and every zone modelled is user-specific. Further investigation is still required to properly mark out the effect of modification on specific engine parameters.

5. The use of ethanol in the internal combustion engine has given better results of engine performance with promising encouraging effect on emission fraction as compared to that of the gasoline standard.

REFERENCES

[1]   Yan B, Wang H, Zheng Z, Qin Y, Yao M. (2018) The effect of combustion chamber geometry on in-cylinder flow and combustion process in a stoichiometric operation natural gas engine with EGR. Applied Thermal Engineering, 129: 199-211.

[2]   Evans RL. (1992) Combustion chamber design for a lean-burn SI engine. SAE Transactions, 1611-1616.

[3]   Wohlgemuth S, Roesler S, Wachtmeister G. (2014) Piston design optimization for a two-cylinder lean-burn natural gas engine-3D-CFD-simulation and test bed measurements (No. 2014-01-1326). SAE Technical Paper.

[4]   Evans RL, Tippett EC. (1990) The effects of squish motion on the burn-rate and performance of a spark-ignition engine (No. 901533). SAE Technical Paper.

[5]   Jones MK, Heaton DM. (1989) Nebula combustion system for lean burn spark ignited gas engines (No. 890211). SAE Technical Paper.

[6]   Sakurai T, Iko M, Okamoto K, Shoji F. (1993) Basic research on combustion chambers for lean burn gas engines. SAE Transactions, 2240-2250.

[7]   Johansson B, Olsson K. (1995) Combustion chambers for natural gas SI engines part I: Fluid flow and combustion. SAE Transactions, 374-385.

[8]   Olsson K, Johansson B. (1995) Combustion chambers for natural gas SI engines part 2: Combustion and emissions. SAE transactions, 499-511.

[9]   Masoudi R, Azad NL, McPhee J. (2014) Parameter identification of a quasi-dimensional spark-ignition engine combustion model (No. 2014-01-0385). SAE Technical Paper.

[10] Kaprielian L, Demoulin M, Cinnella P, Daru V. (2013) Multi-zone quasi-dimensional combustion models for Spark-Ignition engines (No. 2013-24-0025). SAE Technical Paper.

[11] Juntarakod P, Soontornchainacksaeng T. (2014) A quasi-dimensional three-zone combustion model of the diesel engine to calculate performances and emission using the diesel-ethanol dual fuel. Eng. Sci, 7(1): 19-37.

[12] Sánche ÓJ, Cardona CA. (2012) Conceptual design of cost-effective and environmentally-friendly configurations for fuel ethanol production from sugarcane by knowledge-based process synthesis. Bioresource Technology, 104: 305-314.

[13] Alamu OJ, Waheed MA, Jekayinfa SO. (2007) Biodiesel production from Nigerian palm kernel oil: effect of KOH concentration on yield. Energy for Sustainable Development, 11(3): 77-82.

[14] Gnansounou E, Dauriat A. (2005) Ethanol fuel from biomass: A review. CSIR, 64 (11): 809-821. http://hdl.handle.net/123456789/5372

[15] Yücesu HS, Sozen A, Topgül T, Arcaklioğlu E. (2007) Comparative study of mathematical and experimental analysis of spark ignition engine performance used ethanol–gasoline blend fuel. Applied Thermal Engineering, 27(2-3): 358-368.

[16] Ceviz MA, Yüksel F. (2005) Effects of ethanol–unleaded gasoline blends on cyclic variability and emissions in an SI engine. Applied Thermal Engineering, 25(5-6): 917-925.

[17] Verma AP, Choube A. (2012) Ethanol as alternative fuel for SI engine - A review. 4(14): 90-95.

[18] Srinivasan CA, Saravanan CG. (2010) Study of combustion characteristics of an SI engine fuelled with ethanol and oxygenated fuel additives. Journal of Sustainable Energy & Environment, 1: 85-91.

[19] Taraba JL, Turner GM, Razor R. (1981) Energy in agriculture: The use of ethanol as an unmixed fuel for lnternal combustion engines. AEES, 14(8): 1-20

[20] Park IJ, Yoo YH, Kim JG, Kwak DH, Ji, WS. (2011) Corrosion characteristics of aluminum alloy in bio-ethanol blended gasoline fuel: Part 2. The effects of dissolved oxygen in the fuel. Fuel, 90(2): 633-639.

[21] Larsen U, Johansen T, Schramm J. (2009) Ethanol as a future fuel for road transportation: Main research report. DTU Mekanik,

[22] Yoo YH, Park IJ, Kim JG, Kwak DH, Ji WS. (2011) Corrosion characteristics of aluminum alloy in bio-ethanol blended gasoline fuel: Part 1. The corrosion properties of aluminum alloy in high temperature fuels. Fuel, 90(3): 1208-1214.

[23] Strong, RM. (1911). Gasoline and alcohol tests on internal-combustion engines (No. BM-BULL-32). Bureau of Mines, Washington, DC (USA).

[24] Bhetalu AD, Patil SS, Ingole NW. An overview ethanol as a motor fuel. Journal of Engineering Research and Studies, 3(2): 50-53.

[25] Bokhary AYF, Alhazmy M, Ahmad N, Albahkali A. (2014) Investigations on the utilization of ethanol-unleaded gasoline blends on SI engine performance and exhaust gas emission. International Journal of Engineering & Technology, 14(2): 88-96.

[26] Karavalakis G, Durbin TD, Shrivastava M, Zheng Z, Villela M, Jung H. (2012) Impacts of ethanol fuel level on emissions of regulated and unregulated pollutants from a fleet of gasoline light-duty vehicles. Fuel, 93: 549-558.

[27] Yusaf T, Buttsworth D, Najafi G. (2009) Theoretical and experimental investigation of SI engine performance and exhaust emissions using ethanol-gasoline blended fuels. In 2009 3rd International Conference on Energy and Environment (ICEE) (pp. 195-201). IEEE.

[28] Kumar, J, Trivedi, D, Mahara, P, Butola, R. (2013). Performance study of ethanol blended gasoline fuel in spark ignition engine. Journal of Mechanical and Civil Engineering, 7(3): 71-78.

[29] Pai S, Tasneem HA, Rao A, Shivaraju N, Sreeprakash B. (2013) Study of impact of ethanol blends on SI engine performance and emission. National Conference on Challenges in Research & Technology in the Coming Decades CP648, pp 1-7.

[30] De Simio L, Gambino M, Iannaccone S. (2012) Effect of ethanol content on thermal efficiency of a spark-ignition light-duty engine. International Scholarly Research Network Renewable Energy, 2012(219703): 1-8.

[31] Dare AA, Ismail OS, Olatunde OB. (2017) Development of three-zone transitional model for reciprocating internal combustion engine analysis using gasoline. Current Journal of Applied Science and Technology, 25(6): 1-11.

[32] Dare AA, Olatunde OB. (2018) Development of four-zone segmented transitional model for reciprocating internal combustion engine analysis using gasoline. American Journal of Science, Engineering and Technology, *3*(2): 46-52.

[33] Buttsworth DR. (2002) Spark ignition internal combustion engine modelling using Matlab. Faculty of engineering & surveying technical reports TR-2002-02: 1-41.

[34] Ferguson CR, Kirkpatrick AT. (2016) Internal combustion Engine. Applied Thermosciences. Third Edition. John Wiley & Sons, Ltd.

[35] Kodavasal J, Keum S, Babajimopoulos A. (2011) An extended multi-zone combustion model for PCI simulation. Combustion Theory and Modelling, 15(6): 893-910.

[36] Asgari O, Hannani SK, Ebrahimi R. (2012) Improvement and experimental validation of a multi-zone model for combustion and NO emissions in CNG fueled spark ignition engine. Journal of Mechanical Science and Technology, *26*(4): 1205-1212.

[37] Heywood JB. (1988) *Internal Combustion Engine Fundamentals*. McGraw Hill, Inc. New York series (11) pp.1